



ELSEVIER

Polymer 43 (2002) 7461–7465

polymerwww.elsevier.com/locate/polymer

Light scattering studies on crystallization in polyethylene terephthalate

Daisuke Tahara^{a,*}, Koji Fukao^{b,1}, Yoshihisa Miyamoto^b^aGraduate School of Human and Environmental Studies, Kyoto University, Kyoto 606-8501, Japan^bFaculty of Integrated Human Studies, Kyoto University, Kyoto 606-8501, Japan

Received 18 April 2002; received in revised form 9 August 2002; accepted 9 September 2002

Abstract

The light scattering from the spherulites of polyethylene terephthalate grown near the glass transition temperature has been investigated. The Hv scattering profiles can be reproduced by the sum of the ideal spherulite scattering with the distribution of spherulite radius and the isotropic scattering from randomly oriented crystallites. The ratio of optical anisotropies in the isotropic scattering to the ideal spherulite scattering is obtained by the method established to eliminate the effects of the number density of spherulites and the coefficient depending on the experimental conditions. It is found that the anisotropy ratio is almost independent of the crystallization time and of temperature above 106 °C, while it is larger at a crystallization temperature of 103 °C. The spherulitic structure is discussed in terms of the anisotropy ratio. © 2002 Elsevier Science Ltd. All rights reserved.

Keywords: Light scattering; Polyethylene terephthalate; Spherulite

1. Introduction

Light scattering is a suitable method for investigating the internal structure of a polymer spherulite, since it gives the information of the structure in the scale of the order of μm . This method is also applied to the analyses of the spherulitic structure formation in the early stage of crystallization [1–3]. In these studies, however, the analyses were made in terms of the integrated intensity and the peak position of scattering profile, but no detailed analysis of scattering profile was made. In polyethylene terephthalate (PET), the changes in structure and dynamics are reported before the crystalline structure is formed at temperatures near the glass transition temperature T_g [1,4–6]. In order to investigate the early stage of spherulite formation process, the profile of light scattering intensity must be examined in detail. In this study, the scattering intensity profiles are carefully analysed in the growth process of spherulite near T_g focusing on the Hv scattering, which will be served as a basis of the examination of the structure in the early stage of spherulite formation.

The light scattering profiles have been studied for many years. What is called a four-leaf clover scattering pattern

typically observed on Hv scattering from spherulites was qualitatively explained by the ideal spherulite model [7], and the observed intensities of Hv light scattering from the spherulites of isotactic polystyrene (iPS) and isotactic polypropylene (iPP) were quantitatively reproduced by the sum of the intensity of the ideal spherulite and that of crystallites oriented randomly (isotropic scattering) [8,9]; the latter is independent of the azimuthal scattering angle and supposed to originate from an orientation correlation between crystallites. Since the observed absolute scattered intensities depend on the experimental conditions such as the sample thickness and its distribution, the surface conditions of the sample, etc., it is difficult, depending on the material, to compare the results obtained under the different conditions. In this paper, firstly the Hv scattering patterns are quantitatively reproduced based on Keijzers' combination model [8], taking account of the distribution of spherulite radius. Secondly the method is presented to obtain the ratio of the optical anisotropy of spherulite to that of crystallite attributable to the isotropic scattering, and the change in spherulitic structure with crystallization temperature and time is discussed.

2. Experimental section

The material used was PET kindly supplied by Toyobo

* Corresponding author. Tel.: +81-75-753-6775; fax: +81-75-753-6805.
E-mail address: tahara@phys.h.kyoto-u.ac.jp (D. Tahara).

¹ Present address: Department of Polymer Science and Engineering, Kyoto Institute of Technology, Matsugasaki, Kyoto 606-8585, Japan.

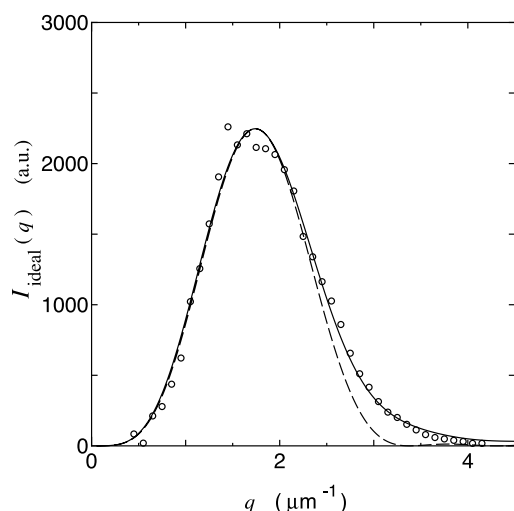


Fig. 1. The intensity profile of the ideal spherulite at $T_c = 106^\circ\text{C}$ and $t_c = 3890$ s. The broken line is given by Eq. (1) which has the same peak intensity as the observed one. The solid line is obtained from Eq. (2) with $R_{\max} = 2.6 \mu\text{m}$.

Co. Ltd ($M_w = 5.97 \times 10^3$, $M_w/M_n = 2.51$). The film specimens about $30 \mu\text{m}$ thick were prepared by pressing the pellets between cover glasses at 310°C for 3 min and then quenched in an ice–water bath to obtain an amorphous specimen (T_g of this material is about 75°C). The melt-quenched specimen was quickly inserted into a hot chamber kept at a desired crystallization temperature T_c and the isothermal crystallization at T_c was investigated by time-resolved light scattering. The range of T_c studied is from 103 to 123°C . A light source was a polarized He–Ne laser of 632.8 nm wavelength and the diameter of the beam is 0.8 mm. The scattered light passed through an analyser was projected onto a screen, and the two-dimensional scattered intensity was measured by a CCD camera. The linearity between the scattered light intensity and the observed one has been confirmed within the measured range of the intensity.

3. Results and discussion

The Hv light scattering pattern from PET spherulites shows a four-leaf-clover pattern which is typical in the light scattering of polymer spherulites. The intensity of Hv scattering from the ideal spherulite $I_{\text{ideal}}(q, \mu)$ is given by Ref. [7]

$$I_{\text{ideal}}(q, \mu) = Cnv^2 \left(\frac{3}{U^3} \right)^2 [(\alpha_r - \alpha_t) \cos^2 \theta \sin 2\mu \times (4 \sin U - U \cos U - 3SiU)]^2, \quad (1)$$

where q is the magnitude of a scattering vector, μ , the azimuthal angle, C , the constant coefficient depending on the experimental conditions, n , the number of spherulites, θ , a polar scattering angle, v , the volume of a spherulite, α_r and

α_t , the polarizability along the radial direction and along the tangential direction, respectively, $U = (4\pi R/\lambda) \sin(\theta/2) = qR$, $SiU = \int_0^U (\sin x/x) dx$, R , the radius of a spherulite, and λ , the wavelength of the incident light. The azimuthal angle dependence of observed intensity can be expressed by the sum of the intensity proportional to $\sin^2 2\mu$ and that independent of μ . Since $I_{\text{ideal}}(q, \mu = 0^\circ) = 0$, the scattering intensity at $\mu = 0^\circ$ is attributable to that from the randomly oriented crystallites (isotropic scattering), and the intensity component proportional to $\sin^2 2\mu$ to that from the spheres with the radial symmetry of polarizabilities (spherulite scattering component) [8,9]. The dependence of the spherulite scattering component on the scattering vector at $T_c = 106^\circ\text{C}$ and $t_c = 3890$ s is shown in Fig. 1. The optical microscopy could not clearly reveal the individual spherulites because of their small size and three-dimensional overlapping of the spherulites in the field of view, though the rough estimate of the spherulite density was possible. From the beam size and the sample thickness, the number of spherulites irradiated by the laser beam is estimated to be of the order of 10^5 . In Fig. 1, the calculated result for the ideal spherulite model by Eq. (1) fitted at the peak position and the peak value is shown by the broken line; the observed intensity is larger than the calculated one at high q . This discrepancy can be interpreted by the distribution of radii for PET spherulites. When the distribution of radii is constant between 0 and the maximum radius R_{\max} , the q -dependence of the scattering intensity is given by

$$I_{\text{ideal}}(q, \mu; R_{\max}) = \frac{Cn(\Delta\alpha)^2}{R_{\max}} \int_0^{R_{\max}} v^2 \left(\frac{3}{U^3} \right)^2 [\cos^2 \theta \sin 2\mu \times (4 \sin U - U \cos U - 3SiU)]^2 dR, \quad (2)$$

where $\Delta\alpha = \alpha_r - \alpha_t$ is the anisotropy in polarizability of spheres (spherulite anisotropy). The result by Eq. (2) is shown by the solid line in Fig. 1; agreement with the experimental result is satisfactory. Since the intensity of scattering from a spherulite is proportional to R^6 , the contribution from large spherulites dominates the q -dependence of scattering intensity. Although the assumed radius distribution approximately corresponds to the homogeneous nucleation, domination of large spherulites contribution to the intensity suggests that further examination will be necessary regarding whether the homogeneous nucleation is the case under the present crystallization conditions. In this way, the value of R_{\max} can be obtained by fitting the q -dependence of the observed spherulite intensity component by Eq. (2). Fig. 2 shows the crystallization time t_c dependence of R_{\max} . The radius of the spherulite linearly increases with crystallization time in the early stage of growth process, and the apparent growth rate gradually decreases by the impingement of spherulites. It should be noted that in the case of polyethylene difference between the observed scattering intensity and the calculated result at high q is so large that it cannot be attributable to the distribution of spherulite radius. In this case, the phase

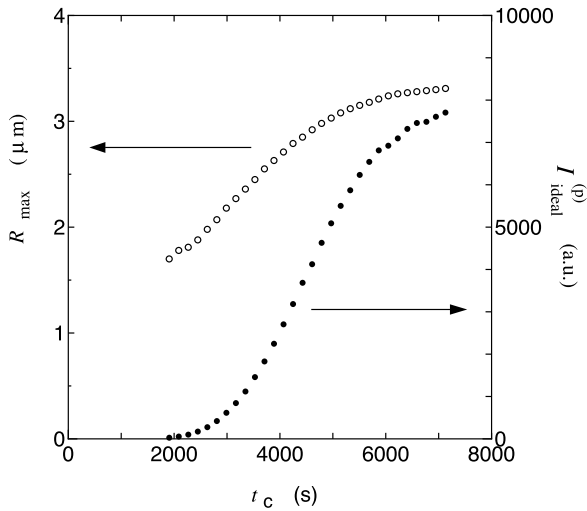


Fig. 2. The crystallization time dependence of the maximum radius R_{\max} (○) and the peak intensity of spherulite scattering (●) at $T_c = 106\text{ }^\circ\text{C}$.

coherence between the isotropic scattering and the scattering from the ideal spherulite is suggested [10].

In the ideal spherulite model, the parameter characterizing the structure of spherulite is the anisotropy of spherulite $\Delta\alpha$, which will be examined as follows. The peak intensity of the scattering profile, $I_{\text{ideal}}^{(p)}$, is obtained from Eq. (2) as

$$I_{\text{ideal}}^{(p)} = 9.53 \times 10^{-3} \left(\frac{4\pi}{3}\right)^2 Cn(\Delta\alpha)^2 R_{\max}^6, \quad (3)$$

where the factor 9.53×10^{-3} appears from the peak value in the integral in Eq. (2). The crystallization time dependence of $I_{\text{ideal}}^{(p)}$ is shown in Fig. 2. Fig. 3 shows the crystallization time dependence of $I_{\text{ideal}}^{(p)}/R_{\max}^6$, which is proportional to $C(\Delta\alpha)^2n$. When the spherulite anisotropy $\Delta\alpha$ remains unchanged with crystallization time, $I_{\text{ideal}}^{(p)}/R_{\max}^6$ is proportional to the number of spherulites n : Fig. 3 shows the number of spherulites increases up to 3500 s at $T_c = 106\text{ }^\circ\text{C}$.

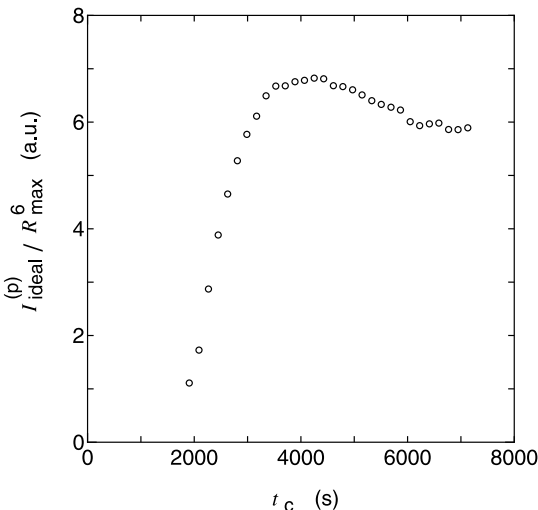


Fig. 3. The crystallization time dependence of $I_{\text{ideal}}^{(p)}/R_{\max}^6$ at $T_c = 106\text{ }^\circ\text{C}$.

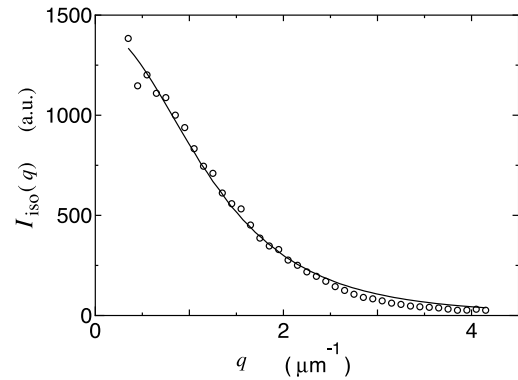


Fig. 4. The intensity profile of the isotropic scattering at $T_c = 106\text{ }^\circ\text{C}$ and $t_c = 3890\text{ s}$. The solid line is fitted by Eq. (4) with $a = 0.54\text{ }\mu\text{m}$.

Since the spherulites become dense and overlap each other in the prolonged crystallization time, the decrease in $I_{\text{ideal}}^{(p)}/R_{\max}^6$ at large t_c will be partly due to multiple scattering.

Next the isotropic scattering is analysed. The scattering intensity at $\mu = 0^\circ$ can be caused by truncation by impingement of spherulites [11]. However, since the isotropic scattering is observed from the early stage of crystallization, the truncation from a spherical shape by impingement of spherulite is not the origin of the isotropic scattering in the present case. When the arrangement of spherulites is random and the number of spherulites is very large, the interference among spherulites is negligible [12]. Thus the isotropic scattering is considered to originate from the orientation correlation between crystallites in a spherulite [8,9]. In this case the size and the number of the objects that give the isotropic scattering are identical to those of the spherulites. We assume that crystallites have a cylindrical symmetry and can be described by two polarizabilities, α_{\parallel} in the principal direction and α_{\perp} perpendicular to this direction. The anisotropy δ is defined by $\delta = \alpha_{\parallel} - \alpha_{\perp}$. Fig. 4 shows the intensity profile of the isotropic scattering component at $T_c = 106\text{ }^\circ\text{C}$ and $t_c = 3890$ (open circles), which is found to be well fitted by the square of Lorentz function (see below). When the exponential decay in the orientation correlation is assumed [8,9,13] and the correlation length is much shorter than the radius of the spherulites, the isotropic scattering intensity is given by

$$I = \frac{32\pi^2}{45} Cn\delta^2 \frac{R^3 a^3}{(1 + (aq)^2)^2}, \quad (4)$$

where a is the correlation length [14]. The observed isotropic intensity $I_{\text{iso}}(q)$ is fitted by Eq. (4) with $a = 0.54\text{ }\mu\text{m}$ (Fig. 4, the solid line). The dependence of the correlation length a on the spherulite radius R_{\max} is shown in Fig. 5 for several crystallization temperatures.

Since the distribution of radii of spherulites is taken into account in the spherulite scattering intensity, the isotropic scattering intensity in this condition is calculated. As reported on iPS spherulites, we consider the case that the correlation length is proportional to radius of the spherulite, that is $a = kR$, where k is a proportional constant ($k \cong 1/6$ in

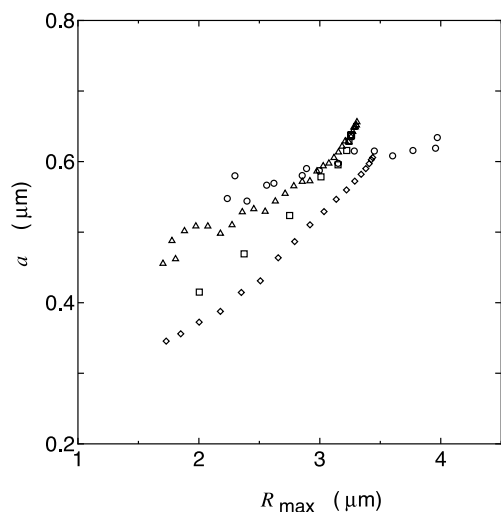


Fig. 5. The relation between the correlation length a and the maximum spherulite radius R_{\max} at $T_c = 103$ (○), 106 (△), 116 (□) and 123 °C (◇).

the case of iPS [9]. When spherulites have the above size distribution and the correlation length of the spherulite with spherulite radius R , $a(R)$, is proportional to R , by averaging in terms of the spherulite radius, the intensity of isotropic scattering is given by

$$I_{\text{iso}}(q, \mu = 0^\circ) = \frac{32\pi^2}{45} C \delta^2 n R_{\max}^3 a_{\max}^3 \frac{a_{\max} q (-15 - 10a_{\max}^2 q^2 + 2a_{\max}^4 q^4) + 15(1 + a_{\max}^2 q^2) \arctan a_{\max} q}{6a_{\max}^7 q^7 (1 + a_{\max}^2 q^2)}, \quad (5)$$

where $a_{\max} = kR_{\max}$ is the correlation length of the largest spherulite. This result numerically shows that the distribution of the radii of spherulites hardly changes the intensity profile and Eq. (5) is well approximated by Eq. (4) by replacing a by $0.87a_{\max}$.

In the case of PET, Fig. 5 shows that the correlation length a deduced from Eq. (4) monotonically increases with R_{\max} , but the linear relation between a and R_{\max} is only approximate. In the further analyses in this study, however, when we calculate the scattering intensity of spherulites with the distribution of spherulite radius, the proportionality between the correlation length $a(R)$ and the spherulite radius R is assumed for convenience. Then in Eq. (5) a_{\max} is substituted with $a/0.870$ and the intensity of the isotropic scattering at $q \rightarrow 0$, $I_{\text{iso}}(0)$, is given by

$$I_{\text{iso}}(0) = 1.52 C n \delta^2 a^3 R_{\max}^3. \quad (6)$$

The value of $I_{\text{iso}}(0)$ is obtained by extrapolating from the observed intensity, and $C n \delta^2$ can be obtained from $I_{\text{iso}}(0)/R_{\max}^3 a^3$. Fig. 6 shows $I_{\text{iso}}(0)/R_{\max}^3 a^3$ as a function of t_c , whose crystallization time development is similar to that of the scattering from the ideal spherulite (Fig. 3).

The scattering patterns can be reproduced by Eqs. (2) and (4) with parameters R_{\max} and a in the range of T_c and t_c studied. The parameters used to characterize a spherulite are the anisotropy of spherulite $\Delta\alpha$ and that of crystallites δ

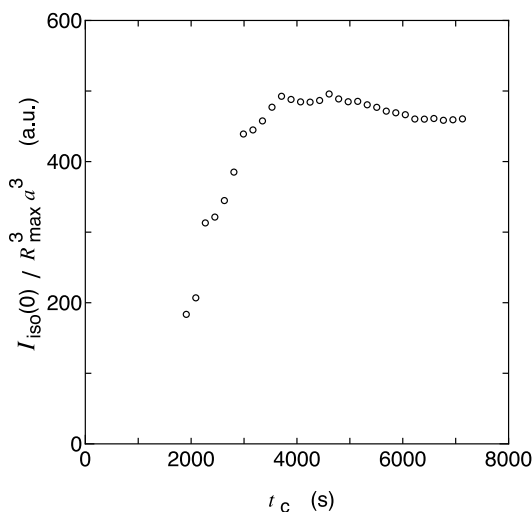


Fig. 6. The crystallization time dependence of $I_{\text{iso}}(0)/R_{\max}^3 a^3$ at $T_c = 106$ °C.

besides R_{\max} and a . In the above analyses we obtained $C n (\Delta\alpha)^2$ and $C n \delta^2$ separately. The coefficient C depends on the condition of the measurement such as the sample thickness, but C is common for the scatterings from the ideal spherulite and the isotropic scattering. From Eqs. (3) and (6)

the anisotropy ratio is given by

$$\left| \frac{\delta}{\Delta\alpha} \right| = \sqrt{0.110 \times \frac{I_{\text{iso}}(0) R_{\max}^3}{I_{\text{ideal}}^{(p)} a^3}}. \quad (7)$$

This equation is valid not only for the spherulites with the distribution of the radii, but also for those without distribution and in the case a is proportional to R if the numerical factor is properly modified.

Fig. 7 shows $\sqrt{0.110 \times (I_{\text{iso}}(0) R_{\max}^3) / (I_{\text{ideal}}^{(p)} a^3)}$ as a function of R_{\max} at several crystallization temperatures. Here the anisotropy ratio is plotted against R_{\max} rather than t_c since the former variable is more suitable when we examine the change in spherulite structure with the growth of spherulites. From the figure, the following features can be found: (a) At each T_c , the anisotropy ratio is nearly constant or slightly increases with the spherulite radius, hence with crystallization time. (b) The anisotropy of crystallite δ is larger than that of the spherulite $\Delta\alpha$ by three to four times. (c) The anisotropy ratio is almost independent of crystallization temperature above $T_c = 106$ °C, while the value at $T_c = 103$ °C is larger than that at other T_c 's.

The result (a) indicates that the structure of spherulites is determined by the crystallization conditions, and the annealing effects during growth is not pronounced, except for the development of the correlation length a . The

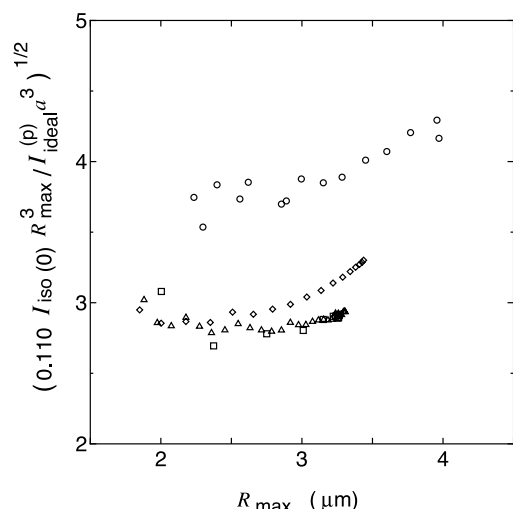


Fig. 7. The dependence of $\sqrt{0.110 \times (I_{\text{iso}}(0) R_{\text{max}}^3) / (I_{\text{ideal}}^{(p)} a^3)}$ on the spherulite radius R_{max} at $T_c = 103$ (○), 106 (△), 116 (□) and 123 °C (◇).

intensity of the Hv scattering of the spherulite crystallized at 103 °C is weaker and less anisotropy is observed under the crossed polarized optical microscope, compared with other crystallization temperatures. This suggests that the difference in anisotropy ratio between crystallization temperatures (result (c)) can be attributable to the decrease in $\Delta\alpha$ rather than the increase in δ at $T_c = 103$ °C. These results indicate that less ordered spherulites are formed at crystallization temperatures near T_g . The crystallite and the spherulite are aggregates of single crystals. In particular, the origin, the structure and the spatial distribution of crystallites are yet unclarified. The anisotropies of these aggregates should be calculated from the polarizability tensor of single crystal by some orientational averages. Keijzers et al. referred the ideal spherulite scattering to the spherulitic crystallites formed at the primary crystallization, and the isotropic scattering to the randomly oriented crystallites formed at the secondary crystallization [8]. The constancy of the anisotropy ratio with t_c and T_c in our results, however, suggests that the two anisotropies originate from same crystallites [9,15]: a spherulite is an aggregate of crystallites which have the orientation correlation and have ideal spherulitic symmetry on average. Since the crystallite is considered a much smaller entity than the spherulite, the result (b) is consistent with this consideration and will give important information about the structure of the crystallites and the spherulites. On the other hand, when the same crystallites give the ideal

spherulite scattering and the isotropic scattering, the interference between these two scattering amplitudes should be examined more carefully. The scattering intensity of a two-dimensional spherulite which consists of crystallites which give both the ideal spherulite scattering and the isotropic scattering has been calculated [16]. However, the intensity predicted by this model at $\mu = 0^\circ$ is much smaller than that observed in the experiment. It is necessary to carry out the calculation in three dimension in order to compare the results. A structure model will be required compatible with the combination model and with the crystallite fluctuation model, and detailed analyses on Vv scattering combined with the present Hv scattering will elucidate these issues more clearly.

Acknowledgements

This work is partly supported by a Grant-in-Aid of Japan Society for the Promotion of Science and by a Grant-in-Aid for Science Research on Priority Areas, 'Mechanism of Polymer Crystallization' (Grants Nos. 12127203 and 12127204) from The Ministry of Education, Science, Sports and Culture of Japan.

References

- [1] Lee CH, Saito H, Inoue T. *Macromolecules* 1993;26:6566–9.
- [2] Pogodina NV, Winter HH. *Macromolecules* 1998;31:8164–72.
- [3] Pogodina NV, Siddinquee JW, van Egmond JW, Winter HH. *Macromolecules* 1999;32:1167–74.
- [4] Imai M, Mori K, Mizukami T, Kaji K, Kanaya T. *Polymer* 1993;33:4451–7.
- [5] Imai M, Kaji K, Kanaya T. *Phys Rev Lett* 1993;71:4162.
- [6] Fukao K, Miyamoto Y. *Phys Rev Lett* 1997;79:4613.
- [7] Stein RS, Rhodes MB. *J Appl Phys* 1960;31:1873–84.
- [8] Keijzers AEM, van Aartsen JJ, Prins WJ. *J Am Chem Soc* 1968;90:3107–13.
- [9] Hashimoto M, Toda A, Miyaji H. *Polymer* 1992;33(5):909–13.
- [10] Hashimoto T, Prud'homme RE, Stein RS. *J Polym Sci, Polym Phys Ed* 1973;11:709–36.
- [11] Stein RS, Picot C. *J Polym Sci, A2* 1970;8:2127–39.
- [12] Prud'homme RE, Stein RS. *J Polym Sci, Polym Phys Ed* 1973;11:1357–74.
- [13] Stein RS, Stidham SN. *J Appl Phys* 1964;35(1):42–6.
- [14] Debye P, Anderson HR, Brumberger H. *J Appl Phys* 1957;28(6):679–83.
- [15] Stein RS, Chu W. *J Polym Sci, A2* 1970;8:1137–57.
- [16] Yoon DY, Stein RS. *J Polym Sci, Polym Phys Ed* 1974;12:763–84.